Simulation of Heat Transfer to Separation Air Flow in a Concentric Pipe

C. S. Oon [a, b, *], A. Al-Shamma'a [b], S. N. Kazi [a], B. T. Chew [a], A. Badarudin [a], E. Sadeghinezhad [a]

[a]Department of Mechanical Engineering, Faculty of Engineering, University of Malaya 50603 Kuala Lumpur, Malaysia.

[b]School of Built Environment, Liverpool John Moores University, Byrom Street, Liverpool, L3 3AF, United Kingdom.

* Corresponding author e-mail: oonsean2280@siswa.um.edu.my; oonsean2280@yahoo.com

Abstract: Flow separations occur in various engineering applications. Computational simulation by using standard k-ε turbulence model was performed to investigate numerically the characteristic of backward-facing step flow in a concentric configuration. This research is focused on the variation of Reynolds number, heat flux and step height in a fully developed turbulent air flow. The design consists of entrance tube, inner and outer tubes at the test section. The inner tube is placed along the entrance tube at the test section with an outer tube to form annular conduit. The entrance tube diameter was varied to create step height, s of 18.5 mm. The Reynolds number was set between 17050 and 44545 and heat flux was set between 719 W/m^2 and 2098 W/m^2 respectively. It is observed that the higher Reynolds number with step flow contribute to the enhancement of heat transfer. The reattachment point for q=719 W/m^2 is observed at 0.542 m, which is the minimum surface temperature. The experimental data shows slightly lower distribution of surface temperature compared to simulation data. As for the same case in experimental result, the minimum surface temperature is obtained at 0.55 m. The difference between numerical and experimental result is 0.008 m. Finally, it can be inferred that utilizing the computational fluid dynamic package software, agreeable results could be obtained for the present research.

Keywords: Numerical Simulation; Heat Transfer; Turbulent Flow; Computational Fluid Dynamics; Backward Facing Step

Nomenclature

Re_x Reynolds number

U Velocity of the fluid,

ρ_f Density at film temperature

μ_f Dynamic viscosity at film temperature

X Distance along horizontal axis.

h_x Convection heat flux

T_{sx} Local surface temperature

T_{bx} Local bulk air temperature

q_c Convection heat flux

$T_{out,ave}$ Average outlet temperature

$T_{in,ave}$ Inlet temperature

Nu_x Local Nusselt number

K_f Thermal conductivity.

D_h Turbulent length scale

L Length of the passage

w Width of the passage

k Turbulence kinetic energy

ω Specific dissipation rate

G_k Generation of turbulent kinetic energy

G_ω Generation of specific dissipation rate

T_k Effective diffusivity of k

T_ω Effective diffusivity of ω

Y_k Dissipation of k due to turbulence

Y_ω Dissipation of ω due to turbulence

S_k User-defined source term

S_ω User-defined source term

1. Introduction

One of the challenging types of fluid flow problem, from the perspective of computational fluid dynamics (CFD), is fluid flow involving flow separation and reattachment. Flow separation and reattachment is initiated by a sudden expansion in flow passage, it is also known as backward facing step, which is widely found in many engineering applications. Flow separation on a boundary surface occurs when the flow stream lines (the closest stream line to the boundary surface) breaks or separates away from the boundary surface and then reattach at a different point. If the boundary surface has a finite dimension, then flow separation is expected due to the flow divergence over the downstream edge where the fluid flows away from the surface such as air flow across an airfoil. From the classical concept, viscosity induces flow separation, which is recognized as boundary layer separation [1].

Mixing of low and high thermal fluid happens in the reattachment flow region affects the heat transfer characteristic. Due to this phenomena, convection over forward and backward step geometries have been investigated by researchers [2]. Fig. 1 illustrates the backward facing step in a sudden expanded pipe.

Fig. 1.

In industries, rotating cylindrical surface in annular passage is commonly used. Thus, the knowledge of this type of flow passage has got special attention. The simplest representation of this geometry is an annulus space between two concentric-shaped surfaces [4, 5]. Study of separation and reattachment flow was conducted first in late 1950's. Futher research were extended to various kind of working fluids (i.e. nanofluids), boundary conditions and geometries [6-8]. In the advent of numerical codes and sophisticated instrumentations, the complex flow in and around the recirculation can be investigated. Besides the experimental and theoretical approaches, numerical simulation has established itself as the most practical and viable alternative to study and to understand different engineering problems.

2. Literature review

Numerical simulation is commonly used to investigate the heat transfer effect and characteristics of flow separation in a backward facing step. Many researchers have been working on complex flow separation encountered in engineering application. A lot of flow separation applications were extensively utilized in industry even though there are still lacks of knowledge on the information of the flow around the recirculation zone. Some of the earlier studies have been focused on understanding the parameters which affect the reattachment process in this flow phenomena considering the point of suppresssion and control of separation process. Other studies have added a major emphasis on observation and analysis of such a flow field [9, 10].

A recent study examined the turbulence forced convection heat transfer over double forward facing step in 2006 [11]. The Navier–Stokes and energy equations were solved numerically by Computational Fluid Dynamics techniques. The solutions were obtained by using the commercial FLUENT code which utilizing the finite volume method [12]. Effects of step heights, step lengths and the Reynolds number on heat transfer and fluid flow were investigated. Results showed that the second step can be used as a

control device for both heat transfer and fluid flow. Other researchers focus on experimental study on the effects of sudden contraction and expansion on characteristics of flow and heat transfer in turbulent condition [13, 14].

3. Methodology

3.1. Design description

An experiment was conducted before the numerical simulations to verify the accuracy and reliability of numerical simulation results. Fig. 2 shows the experimental setup conducted by Togun et al. [15]. The experimental investigation was focused on the effect of separation flow on the local and average convection heat transfer. The experimental set-up consists of inner constant diameter center pipe, outer unheated concentric entrance pipe and constant diameter heated concentric pipe at test section. The outer tube of test section was made of aluminium having 83 mm inner diameter and 600 mm heated length, which was subjected to a constant wall heat flux boundary condition. The investigation was performed in a Re range of 17050–44545, heat flux varied from 719 W/m^2 to 2098 W/m^2 and the step height of 18.5 mm, which is d/D = 1.80.

Fig. 2.

3.2. Mesh independent study

Mesh independent study was considered to authenticate the results of numerical data obtained from software GAMBIT and FLUENT. The computational domain was being meshed using GAMBIT software. Three different types of mesh have been created for mesh independent study (Interval size 4, 4.5 and 5). Constant parameter of step height, s=18.5 mm and heat flux, q=2098 W/m^2 is used in this study for Reynolds number between 17050 and 44545.

3.3. Surface Roughness Study

Study of the effect of surface roughness on heat transfer was taken into consideration. The surface of the heated wall is set to the surface roughness data measured by Kazi et al. for different materials commercially available. Then, the models are simulated with same parameters and conditions to study

the effect of surface roughness. Reynolds number of 17050 and heat flux of 2098 W/m^2 was considered in this case. Table I shows roughness height for different materials.

Table 1

3.4. Data analysis method

The following section will discuss about the equations employed in the numerical simulation. The equations enable researcher to the evaluate heat transfer to the flowing air in an expanded annular passage while the test tube is subjected to uniform wall heat flux.

The local Reynolds number based on the distance (Re_x) can be calculated by Eq. (1):

$$Re_x = \frac{\rho_f \cdot U \cdot X}{\mu_f} \tag{1}$$

where U is the velocity of the fluid, ρ_f is the density at film temperature, μ_f is the dynamic viscosity at film temperature and X is the distance along horizontal axis.

The convection heat flux is used to calculate the local and average heat transfer coefficient as shown by Eq. (2):

$$h_x = \frac{q_c}{(T_{sx} - T_{bx})} \tag{2}$$

where T_{sx} is the local surface temperature, T_{bx} is the local bulk air temperature and q_c is the convection heat flux.

The average of inlet and outlet temperatures are used in finding the local bulk air temperature as shown in Eq. (3):

$$T_{bx} = \frac{(T_{out,ave} + T_{in,ave})}{2} \tag{3}$$

where $T_{out,ave}$ is the average outlet temperature and $T_{in,ave}$ is the inlet temperature, which is assumed at 300 K, the room temperature.

The local Nusselt number based on the distance (Nu_x) can be calculated by Eq. (4):

$$Nu_x = \frac{h_x \cdot X}{K_f} \tag{4}$$

where K_f is the thermal conductivity. The thermal conductivity of air is 0.02 W/m.K.

Turbulent length scale, D_h can be calculated based on the dimension of the passage, as in Eq. (5):

$$D_h = \frac{4 \cdot L \cdot w}{2L \cdot w} \tag{5}$$

where L is the length of the passage, and w is the width of the passage.

The turbulence kinetic energy, k and the specific dissipation rate, ω are obtained from the transport equations, Eq. (6) and Eq. (7):

$$\frac{\partial}{\partial t}(\rho k) + \frac{\partial}{\partial x_i}(\rho k u_i) = \frac{\partial}{\partial x_j}\left(\Gamma_k \frac{\partial k}{\partial x_j}\right) + G_k - Y_k + S_k \tag{6}$$

$$\frac{\partial}{\partial t}(\rho \omega) + \frac{\partial}{\partial x_i}(\rho \omega u_i) = \frac{\partial}{\partial x_j}\left(\Gamma_\omega \frac{\partial \omega}{\partial x_j}\right) + G_\omega - Y_\omega + S_\omega \tag{7}$$

Where G_k is the mean velocity gradients of the turbulent kinetic energy generation. G_ω is the generation of ω. T_k and T_ω represent the effective diffusivity of k and ω, respectively. Y_k and Y_ω represents the dissipation of k and ω due to turbulence. S_k and S_ω are user-defined source terms.

3.5. Computational fluid dynamic

The analysis of the backward-facing step flow was performed by using FLUENT 6.3.26. At four different Reynolds numbers, *Re*=17050, 30720, 39992 and 44545, simulation were conducted at fully developed turbulent unsteady flow where heat flux applied at the outer pipe varied from q = (719, 968, 1458 and 2098) W/m^2. 2nd–order implicit unsteady formulation with pressure based solver is used in the simulation and standard k-epsilon equation was chosen in this case [17]. Second order upwind was selected to solve the momentum, turbulent dissipation rate, energy discretization and turbulent kinetic energy. The mass conservation and momentum equations were linked together through pressure correction by using SIMPLE algorithm [18, 19]. This algorithm offers computational robustness and efficiency in iterating the coupled parameters and higher order differencing schemes. The boundary

condition of the inlet is defined as velocity inlet, the outlet is define as pressure outlet, turbulent intensity 7 % and turbulent length scale 0.06 m. Fluid material is air with density of 1.225 kg/m^3, C_p=1006.43 J/kg-K, thermal conductivity 0.0242 (W/m-K) and viscosity 1.7894x10^{-5}(kg/m-s). Gravity influence is neglected. Table 2 shows the parameters of the numerical simulation.

Table 2

4. Results and discussions

Fig. 3 shows the vectors of air flow passes through the test pipe for a specific case of *Re*=17050, *s*=18.5 mm and *q*=2098 W/m^2. Backward-facing step flow phenomenon appears behind the step, when the flow is separated after passes through the entrance of the test pipe. Lowest temperature region (arrows with yellow color) appears in front of the recirculation region, and it is expected to be the reattachment point, where the heat transfer is maximum. Thus, reattachment point can be detected by finding the axial position of the lowest temperature.

Fig. 3.

The result of mesh independent study utilizing fixed parameter of step height, *s*=18.5 mm and heat flux, *q*=2098 W/m^2 is obtained for Reynolds number between 17050 and 44545. Average heat transfer coefficient is being compared for different interval sizes in fig. 4. Interval size of 4.5 shows the reference among all the numerical data. Interval size of 4 and 5 show errors of 2.44 % and 9.76 % respectively compared to interval size of 4.5 at Reynolds number=39992. Same trend is applied for the Reynolds number of 30720 and 44545. Finally, the deviation of numerical data for Reynolds number=17050 is not significant among the three interval sizes. It can be concluded that the interval sizes of 4 and 4.5 are preferable meshing for heat transfer coefficient investigation in the present case. Fig. 5 shows the increase in surface roughness has no or negligible effect on the average temperature in the simulations.

Fig. 4.

Fig. 5.

Fig. 6 shows variation of the surface temperature with axial distance at different heat fluxes for *s*=18.5 mm and *Re*=44545. The general pattern represents a reduction of the surface temperature when fluid entering the test pipe, just after the step. The surface temperature decreases until it reaches the minimum and then increases gradually and exponentially until the end of the test pipe. The minimum magnitude of temperature is obtained at a specific axial position, where the flow reattachment happens. Increasing of heat fluxes proportionally increases the surface temperature. The lowest heat flux i.e. q=719 W/m^2 shows the lowest surface temperature distribution compared to others, and the highest heat flux i.e. q=2098 W/m^2 provides the highest surface temperature distribution. The reattachment point for q=719 W/m^2 is observed at 0.542 m, which is the minimum surface temperature. The experimental data shows slightly lower distribution of surface temperature compared to simulation data. As for the same case in experimental result, the minimum surface temperature is obtained at 0.55 m. The difference between numerical and experimental result is 0.008 m which is reasonably close. Moreover, the error of average surface temperature between numerical and experimental data is 0.7 %. Base on the distance of reattachment point and average surface temperature for both numerical and experiment result, it can be concluded that the numerical simulation in this case reliable in predicting the heat transfer in flow separation.

Fig. 6.

The evaluated Nusselt numbers for different Reynolds numbers are plotted in fig. 7. Suddent increase in Nusselt number is observed at the end of the recirculation area where reattachment happens. This phenomena is due to intervallic vortex shedding, incoming fluid emptying and filling the recirulation area as suggested by Charwat et al. [10]. The magnitude of Nusselt number and location of reattachement point for Reynolds number 17,505 is agreeable for both simulation and experimental results. Finally, the average Nusselt number errors of less than 10 % is obtained for this case.

Fig. 7.

5. Conclusion

To conclude, the mesh independent study shows good agreement in achieving average surface temperature along the test pipe. The increase in surface roughness has no or neglegible effect on the

average temperature in the simulations. The increase of flow velocity reduces the surface temperature along the pipe to a minimum point then increases through the rest of the pipe. The minimum surface temperature is obtained at flow reattachment point. In the recirculation zone, the Nusselt number improves until it reaches a maximum value at the reattachment point. Generally, the local Nusselt number increases with the increase of the Reynolds number. Thus, it can be inferred that utilizing the computational fluid dynamic package software (Fluent), agreeable results could be obtained for the present investigation.

6. Acknowledgment

This research has been financially supported by High Impact Research Grant UM.C/625/1/HIR/MOHE/ENG/46, UMRG RP012B-13AET and the PPP grant PV145/2012A, University of Malaya, Malaysia for support to conduct this research work.

7. References

[1] P.K. Chang, Control of flow separation, New York: McGraw-Hill, 1976.

[2] H.I. Abu-Mulaweh, A review of research on laminar mixed convection flow over backward- and forward-facing steps, International Journal of Thermal Sciences, 42(9) (2003) 897-909.

[3] C.S. Oon, H. Togun, S.N. Kazi, A. Badarudin, M.N.M. Zubir, E. Sadeghinezhad, Numerical simulation of heat transfer to separation air flow in an annular pipe, International Communications in Heat and Mass Transfer, 39(8) (2012) 1176-1180.

[4] A. Murata, K. Iwamoto, Heat and fluid flow in cylindrical and conical annular flow-passages with through flow and inner-wall rotation, International Journal of Heat and Fluid Flow, 32(2) (2011) 378-391.

[5] M.H. Matin, I. Pop, Numerical Study of Mixed Convection Heat Transfer of a Nanofluid in an Eccentric Annulus, Numerical Heat Transfer, Part A: Applications, 65(1) (2013) 84-105.

[6] M. Rahgoshay, A.A. Ranjbar, A. Ramiar, Laminar pulsating flow of nanofluids in a circular tube with isothermal wall, International Communications in Heat and Mass Transfer, 39(3) (2012) 463-469.

[7] H.A. Mohammed, A.A. Al-aswadi, H.I. Abu-Mulaweh, N.H. Shuaib, Influence of nanofluids on mixed convective heat transfer over a horizontal backward-facing step, Heat Transfer—Asian Research, 40(4) (2011) 287-307.

[8] N.A. Malamataris, A numerical investigation of wall effects in three-dimensional, laminar flow over a backward facing step with a constant aspect and expansion ratio, International Journal for Numerical Methods in Fluids, 71(9) (2013) 1073-1102.
[9] V.I. Terekhov, M.A. Pakhomov, Predictions of turbulent flow and heat transfer in gas–droplets flow downstream of a sudden pipe expansion, International Journal of Heat and Mass Transfer, 52(21–22) (2009) 4711-4721.
[10] İ. Kurtbaş, The effect of different inlet conditions of air in a rectangular channel on convection heat transfer: Turbulence flow, Experimental Thermal and Fluid Science, 33(1) (2008) 140-152.
[11] I.l. Yılmaz, H.F. Öztop, Turbulence forced convection heat transfer over double forward facing step flow, International Communications in Heat and Mass Transfer, 33(4) (2006) 508-517.
[12] C.S. Oon, H. Togun, S.N. Kazi, A. Badarudin, E. Sadeghinezhad, Computational simulation of heat transfer to separation fluid flow in an annular passage, International Communications in Heat and Mass Transfer, 46(0) (2013) 92-96.
[13] H.A. Mohammed, P. Gunnasegaran, N.H. Shuaib, Influence of channel shape on the thermal and hydraulic performance of microchannel heat sink, International Communications in Heat and Mass Transfer, 38(4) (2011) 474-480.
[14] P. Koutmos, C. Mavridis, A computational investigation of unsteady separated flows, International Journal of Heat and Fluid Flow, 18(3) (1997) 297-306.
[15] H. Togun, Y.K. Salman, H.S. Sultan Aljibori, S.N. Kazi, An experimental study of heat transfer to turbulent separation fluid flow in an annular passage, International Journal of Heat and Mass Transfer, 54(4) (2011) 766-773.
[16] S.N. Kazi, G.G. Duffy, X.D. Chen, Mineral scale formation and mitigation on metals and a polymeric heat exchanger surface, Applied Thermal Engineering, 30(14–15) (2010) 2236-2242.
[17] V. Yakhot, S.A. Orszag, S. Thangam, T.B. Gatski, C.G. Speziale, Development of turbulence models for shear flows by a double expansion technique, Physics of Fluids A: Fluid Dynamics (1989-1993), 4(7) (1992) 1510-1520.
[18] D. Lee, J. Lee, H. Park, M. Kim, Experimental and numerical study of heat transfer downstream of an axisymmetric abrupt expansion and in a cavity of a circular tube, Journal of Mechanical Science and Technology, 25(2) (2011) 395-401.

[19] S.V. Patankar, D.B. Spalding, A calculation procedure for heat, mass and momentum transfer in three-dimensional parabolic flows, International Journal of Heat and Mass Transfer, 15(10) (1972) 1787-1806.

Figure Caption

Fig. 1. Schematic diagram for backward facing step [3].

Fig. 2. Dimension of the annular passage in experiment setup [15].

Fig. 3. The vector of air flows in the test section.

Fig. 4. Graph of average heat transfer coefficient versus Reynolds numbers.

Fig. 5. Graph of average temperature versus roughness height for different materials.

Fig. 6. Graph of surface temperature versus distance.

Fig. 7. Graph of Nusselt number versus x/D.

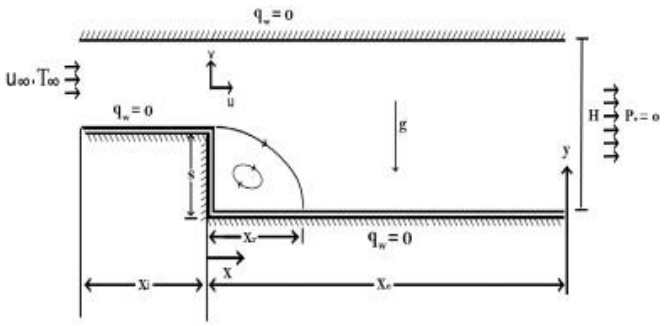

Fig. 1. Schematic diagram for backward facing step [3].

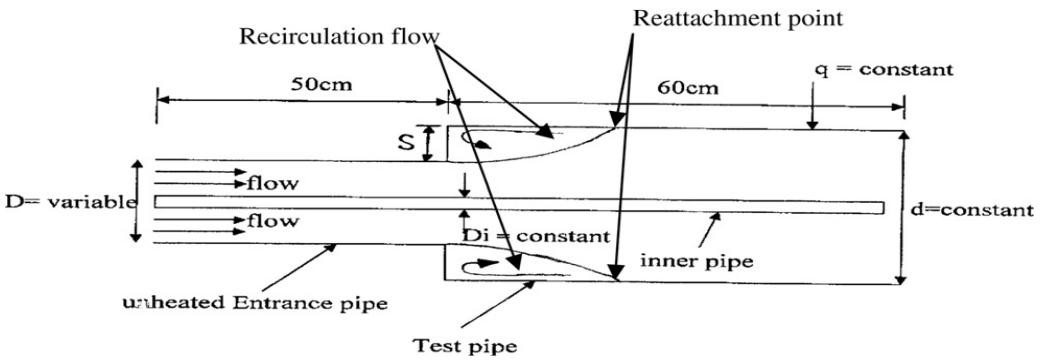

Fig. 2. Dimension of the annular passage in experiment setup [15].

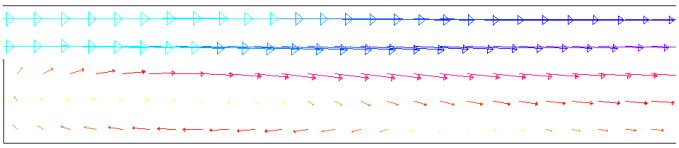

Fig. 3. The vector of air flows in the test section.

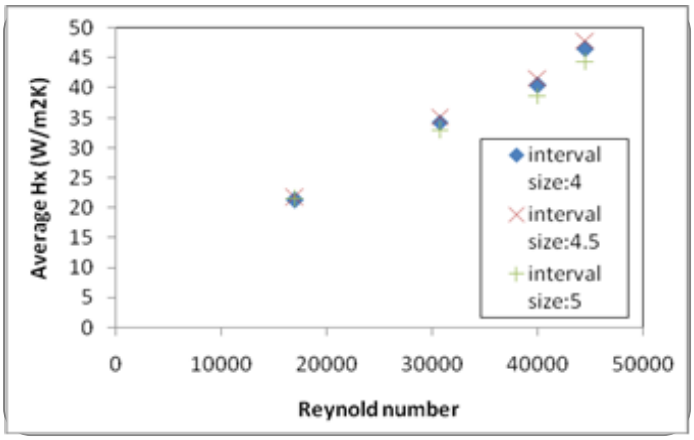

Fig. 4. Graph of average heat transfer coefficient versus Reynolds numbers.

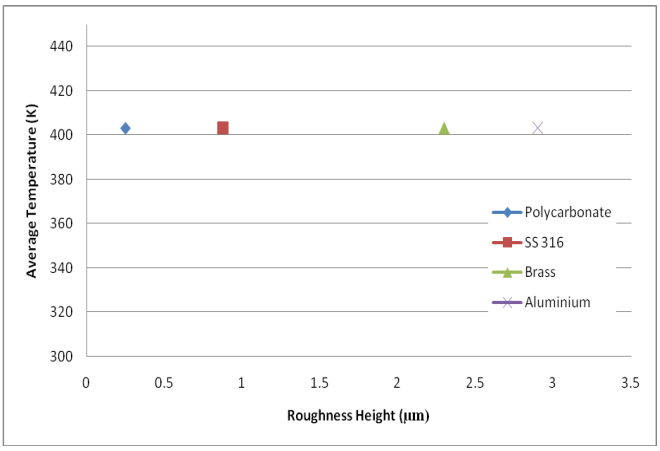

Fig. 5. Graph of average temperature versus roughness height for different materials.

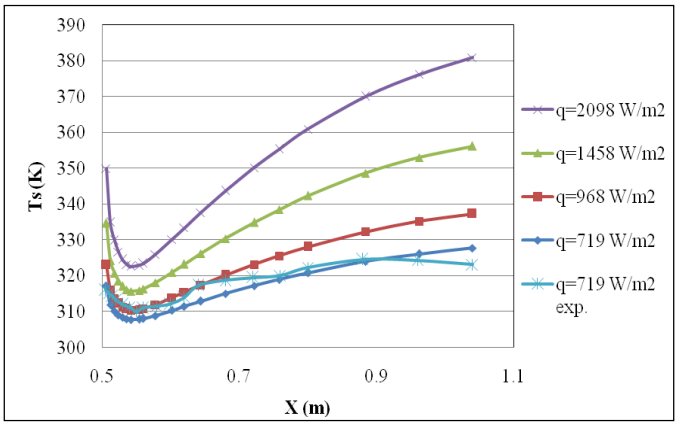

Fig. 6. Graph of surface temperature versus distance.

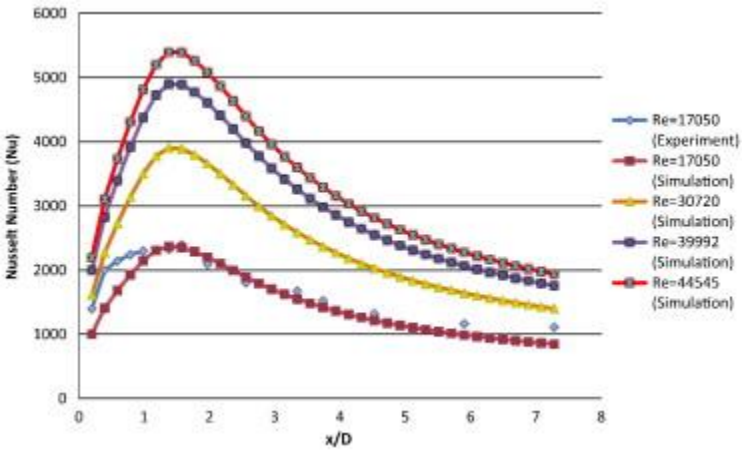

Fig. 7. Graph of Nusselt number versus x/D.

Table Caption

Table 1 Roughness height of the commercially available materials [16].

Table 2 Numerical simulation parameters.

Table 1 Roughness height of the commercially available materials [16].

Specimen	**Roughness Height, µm**
Polycarbonate	0.25
SS 316	0.88
Brass	2.3
Aluminium	2.9

Table 2 Numerical simulation parameters.

Maximum X	1.1 m	**Pressure-Velocity Coupling**	SIMPLE
Maximum Y	0.0305 m	**Discretization (momentum)**	2^{nd} Order Upwind
Space/Time	2D/Unsteady, 2^{nd} Order Implicit	**Discretization (turbulence)**	2^{nd} Order Upwind
Viscous model	k–epsilon, standard	**Residual error**	1×10^{-3}
Material	Air	**Inlet Boundary Type**	Velocity Inlet
Density	1.225 kg/m^3	**Outlet Boundary Type**	Pressure Outlet
Viscosity	1.7894×10^{-5} kg/m-s	**Iteration time step size**	0.1 s
Pressure	101,325 Pa	**Number of time steps**	100